

M.T. Kartel<sup>1,2,3</sup>, K.V. Voitko<sup>3</sup>, Y.V. Grebelna<sup>3</sup>, S.V. Zhuravskiy<sup>3</sup>, K.O. Ivanenko<sup>1,4</sup>,  
T.V. Kulyk<sup>3</sup>, S.M. Makhno<sup>1,2,3</sup>, Yu.I. Sementsov<sup>1,2,3</sup>

## CHANGES IN THE STRUCTURE AND PROPERTIES OF GRAPHENE OXIDE SURFACES DURING REDUCTION AND MODIFICATION

<sup>1</sup> Ningbo Sino-Ukrainian New Materials Industrial Technologies Institute  
Kechuang building, N777 Zhongguanroad, Ningbo, 315211, China

<sup>2</sup> Ningbo University of Technology  
No 55-155 Cui Bai Road, Ningbo, 315016, China

<sup>3</sup> Chuiko Institute of Surface Chemistry of National Academy of Sciences of Ukraine  
17 General Naumov Str., Kyiv, 03164, Ukraine, E-mail: ysementsov@ukr.net

<sup>4</sup> Institute of Macromolecular Chemistry of National Academy of Sciences of Ukraine  
48 Kharkivs'ke shose Str., Kyiv, 02160, Ukraine

The aim of the current study was to find changes in the structure and state of the surface of graphene oxide (GO) under the conditions of its reduction and modification by hetero atoms of nitrogen and amino acids. Reduction of GO was performed with hydrazine hydrate (R-GO), doping with nitrogen atoms - urea impregnation and subsequent heat treatment (N-GO), and the surface of GO was modified with sulfur-containing amino acid - L-cysteine by nucleophilic addition (L-GO). The samples obtained were characterized by analytical methods, such as Raman scattering, IR spectroscopy, TPD-mass-spectrometry, dynamic light scattering spectroscopy. The available Raman spectra indicate a defective structure of GO, reduction of GO leads to greater ordering of the structure in relation to GO, nitrating and modification by amino acid - to the opposite effect, a slight deterioration of the structural state. According to the results of IR spectroscopy, also confirmed by TPD-MS, GO has a large number of functional surface groups: (OH), (C=O), (C=C), (C-O-C), (CO-O-CO), (CH). Hydrazine reduction completely hydrophobizes the surface, in the IR spectra there is only a peak at  $\sim 1040\text{ cm}^{-1}$ , which corresponds to CO-O-CO vibrations, with significantly reduced intensity, as well as bands at  $2120$  and  $2300\text{ cm}^{-1}$ , which indicate the aromatic nature of the samples and exist in all GO derivatives. In nitrogen and sulfur-containing samples (L-GO) a new peak of  $\sim 1520\text{ cm}^{-1}$  appears, which corresponds to N-H vibrations in amines. Sulfur-containing derivatives have valence vibrations at  $600\text{ cm}^{-1}$ , which most likely corresponds to S-H bonds. Thus, modification of GO leads to a significant change in its structure and surface chemistry, which in turn affects the capability of the obtained samples to capture free radicals. Previous empirical studies have shown that this property increases in the series L-GO > GO > N-GO > R-GO.

**Keywords:** graphene oxide, structure, surface properties

### INTRODUCTION

Graphite oxide (Fig. 1), formerly called graphite acid, is a compound of carbon, oxygen and hydrogen in variable ratios, which is obtained by treating graphite with strong oxidants and acids [1]. The most oxidized bulk product is a yellow (yellow-white) solid with a C/O ratio between 2.1 and 2.9, which preserves the structure of the graphite layer, but with a much larger and irregular interplanar distance [2, 3].

Solid material spontaneously disperses in basic solutions or can be dispersed by ultrasound in polar solvents, forming monomolecular sheets known as graphene oxide (GO) by analogy with graphene, a single-layer form of graphite [4].

The GO sheets are used to make strong paper-like materials, membranes, thin films and composite materials. Initially, GO was of considerable interest as a possible intermediate for graphene production. Graphene obtained by reducing GO has many chemical and structural defects, which are a problem for some applications, but an advantage for others [5, 6].

Graphite oxide was first prepared by Oxford chemist Benjamin S. Brody in 1859 by treating graphite with a mixture of potassium chlorate and fuming nitric acid [7]. He reported the synthesis of "paper-like foils" with a thickness of 0.05 mm. In 1957, Hammers and Offman developed a safer, faster, and more efficient process called the Hammer method using a mixture of H<sub>2</sub>SO<sub>4</sub>

sulfuric acid, NaNO<sub>3</sub> sodium nitrate, and KMnO<sub>4</sub> potassium permanganate, which is still widely used, often with some modifications [2].

The GO show significant variations in properties dependent on the oxidation degree and the method of synthesis (Fig. 2) [8–9]. For example, the expanded temperature is generally higher for graphite oxide prepared by the Brody method compared to Hammers graphite oxide, a difference of up to 100 °C at the same heating rates [10]. The hydration and solvation properties of Brody and Hammers graphite oxides are also extremely different [11]. A scalable, safe, ultra-fast and environmentally friendly method for the synthesis of pure GO sheets by electrolytic oxidation of graphite with water is reported in [12].

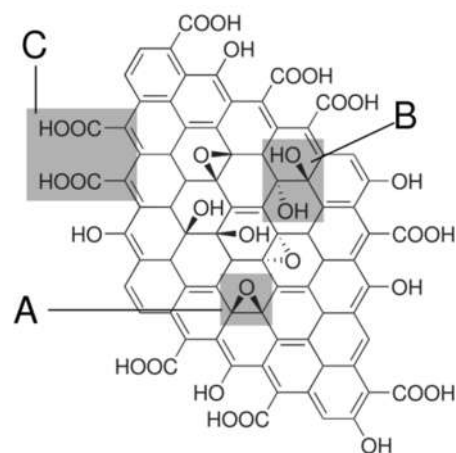


**Fig. 1.** The structure of graphite oxide was proposed in 1998 [1] with functional groups: A-epoxy, B-hydroxyl, C-paired carboxyl groups

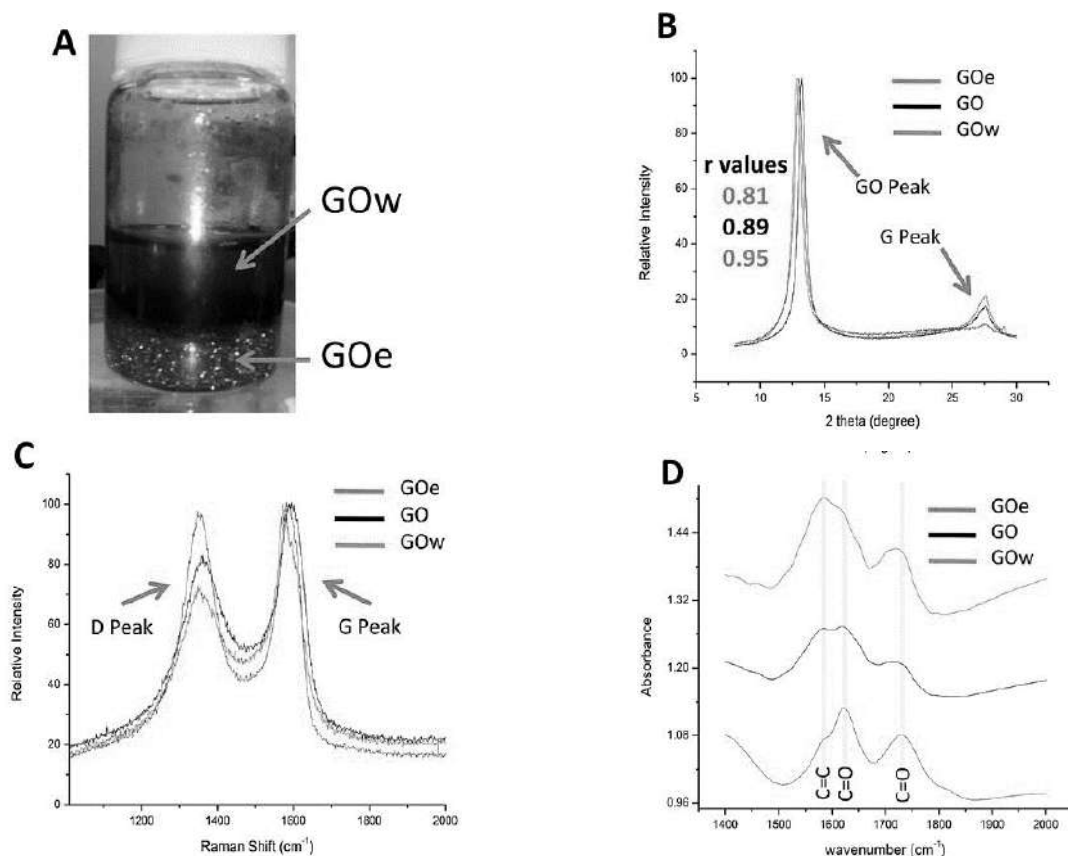


**Fig. 2.** The image of fractionated GO (A); X-ray diffraction patterns (B), Raman (C) and FTIR (D) spectra of GO (black), more oxidized fraction GOw (blue) and less oxidized fraction GOe (red) [8]

Recently it has been found that nanomaterials can imitate antioxidant properties and improve cell survival after ischemia/reperfusion injury (IRI) [13]. The IRI is a pathological condition that occurs in cardiovascular diseases (CVD) caused by the generation of reactive oxygen and nitrogen

species (ROS and RNS) in coronary endothelial or circulating blood cells and cardiomyocytes after a period of ischemia or hypoxia [14].

The unique physicochemical properties of nanomaterials, in particular, large surface area, surface chemistry and targeted drug delivery

allow their use as candidates for biomedical applications. Among them, nanoparticles of metal oxides [15], precious metal materials [16], metal halides [17], hybrid materials [18] showed inherent enzymatic activity.

Carbon nanomaterials can also show the effects of ROS and RNS absorption, which is based on their capability to generate radical adducts at carbon  $sp^2$  sites, transfer surface electrons, and donate hydrogen from functional groups [19, 20].

Due to this, GO has a set of important characteristics and a large surface area is the most important one. In simply way, GO can be considered as a structure where the absorption of radicals will occur by all atoms of material present on the surface. According to the literature, the antioxidant activity of graphene-based materials strongly depends on their electron density, chemical composition,  $sp^2$ -hybridized carbon content and chemical properties.

Therefore, the aim of the current study was to find changes in the structure and surface chemistry of GO under the conditions of its reduction and modification by heteroatoms of nitrogen and amino acid.

## RESULTS AND DISCUSSIONS

**Methods and materials.** Initial GO samples were obtained from “Grafren AB” (Sweden) as a dark brown 20–25 % water-soluble paste, which was synthesized in accordance with ISO/TS 80004-13:2017 (E) “Graphene and related two-dimensional (2D) materials”. According to the certificate: the number of layers is 10–15, the size of the flakes – 0.1–200  $\mu\text{m}$ , the atomic ratio C/O is 2.5–2.6.

Reducing of samples was performed using hydrazine hydrate according to the method specified in [21]. 100 mg of GO was filled with distilled water ( $V = 100$  ml) and dispersed by ultrasound (40 kHz) to obtain a stable suspension without visible agglomerates. Then 10 ml of 99 %  $\text{N}_2\text{H}_4\text{HCl}$  was added and boiled for 24 h in an air-cooled water bath (100 °C) until a black precipitate was obtained in the flask. The precipitate was then filtered and kept in 1 M NaOH for 12 h and then for another 12 h in 1 M HCl. The obtained sample was washed with distilled water to neutral pH and dried at 105 °C for 4 hours (schematically, this process is shown in Fig. 3). Reduced GO samples were designated R-GO.

To obtain nitrogen-containing GO (N-GO) derivatives, a portion of the oxidized sample was immersed in a 10 % urea solution and evaporated to constant weight. After that, additional heat treatment of the sample was performed for 1 h in an inert atmosphere (700–800 °C), then washed with distilled water to neutral pH and dried for 4 hours at 105 °C.

In animal experiments, it has been shown that the introduction of a donor of  $\text{H}_2\text{S}$  (such as NaHS) inhibits the development of oxidative stress in diabetes and renal pathology [22, 23]. In addition, NaHS prevents reperfusion damage to the myocardium during IRI [24]. Therefore, sulfur-derived GO derivatives, in particular GO, modified with the aminoacid *L*-cysteine (*L*-GO) were obtained. For this purpose, 30 mg of GO was dissolved in 60 ml of distilled water and 20 ml of NaOH (pH 10–12). 0.25 g of *L*-cysteine was dissolved in 10 ml of  $\text{H}_2\text{O}$  and added to the pre-prepared suspension of GO at a temperature of 80 °C. Nucleophilic attachment of the aminoacid to the surface of the GO was performed for 12 hours at 80 °C and 12 hours at room temperature. Samples of *L*-GO were washed on a flow unit “Amicon” to obtain a neutral pH filtrate. As a result of the synthesis, 22 mg of sulfur-containing samples were obtained.

Various structural and spectral methods were used to analyze GO samples and their modified forms. The particle size distribution function was determined by dynamic light scattering (DLS) analysis in THF using a laser photon correlation spectrometer Zetasizer-3 (Malvern Instrument, UK). Raman spectra were recorded using a T-64000 Horiba Jobin-Yvon spectrometer in the backscattering geometry at room temperature under excitation with an argon laser ( $\lambda = 488$  nm, 1 mV). Spectra of thermoprogrammed desorption mass spectrometry (TPD-MS) were obtained on a monopole mass spectrometer MX-7304A (Sumy, Ukraine) with electronic beam ionization, adapted for thermo-desorption measurements. The samples (0.1–2 mg) were heated to 750 °C. in a molybdenum/quartz ampoule. FTIR spectra were recorded using an IRTracer 100 (Shimadzu, Japan) using an ATR diamond crystal. The recorded spectra were the result of the joint addition of 20 interferograms obtained with a resolution of 4  $\text{cm}^{-1}$ .

**Structural characteristics of GO, its reduced and modified forms.** The layers of GO have a thickness of about  $1.1 \pm 0.2$  nm. Scanning

tunneling microscopy shows the presence of local regions where oxygen atoms are located perpendicular to the lattice constant of  $0.27 \times 0.41$  nm [25–26]. The edges of each layer are terminated by carboxyl and carbonyl groups [27].

X-ray photoelectron spectroscopy (XPS) shows the presence of several *C1s* peaks, their number and relative intensity dependent on the specific oxidation method used. The attribution of these peaks to certain types of carbon functional groups is somewhat uncertain and is still under discussion. For example, one of the interpretations looks like this: C=C (284.8 eV),

C–O (286.2 eV), C=O (287.8 eV) and O–C=O (289.0 eV) [29]. Another interpretation using the calculation of functional density theory is as follows: C=C with defects such as functional groups and pentagons (283.6 eV), C=C (non-oxygenated rings) (284.3 eV),  $sp^3$  C–H in the basal plane and C=C with functional groups (285.0 eV), C=O and C=C with functional groups, CO (286.5 eV) and OC=O (288.3 eV) [30].

The spectra of Raman scattering and deconvolution of these spectra in the form of Gauss-Lorentz bands after manual subtraction of the baseline of obtained samples are shown in Fig. 4.

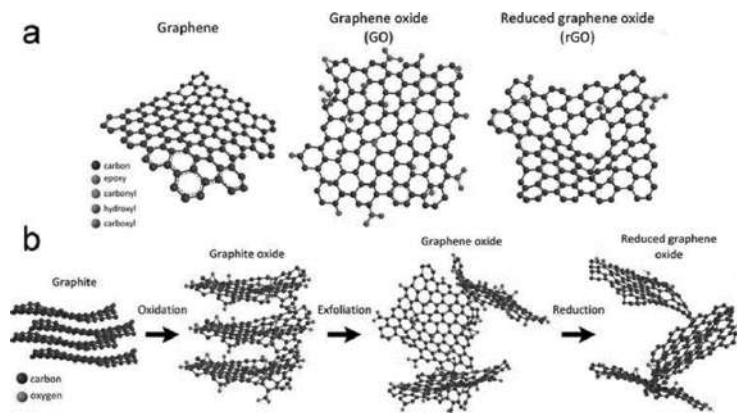


**Fig. 3.** Structures of graphene lattice, graphene oxide (GO) and reduced graphene oxide (R-GO) [28]

The values of the characteristics of typical bands are given in Table. The Raman spectra of GO have a typical appearance (Fig. 4 a). The G-band ( $\sim 1584$   $\text{cm}^{-1}$ ) is shifted in frequency with respect to crystalline graphite and theoretical calculation for an ideal hexagonal lattice ( $1580$   $\text{cm}^{-1}$ ), expanded  $\sim 105$   $\text{cm}^{-1}$ , for graphite  $\sim 20$   $\text{cm}^{-1}$ . A similar change is observed for the D-band:  $1366$   $\text{cm}^{-1}$ , for graphite – absent, for soot –  $1318$   $\text{cm}^{-1}$ , for single-layer CNT –  $1275$   $\text{cm}^{-1}$ , for multilayer CNT –  $1348$   $\text{cm}^{-1}$ . At the frequency  $\sim 1146$   $\text{cm}^{-1}$ , a band corresponding to  $sp^3$ -hybridization (D (-) in the Table) is observed, which explains the experimental “blue” shift of the G-band of the Raman spectra relative to graphite [31–36].

Raman spectra of the second order represent two main broad bands, of which it is considered [32] that it is difficult to identify clearly any of the different components (D+D’, 2D, D+G and 2D’) (Fig. 4). We decided on at least a partial interpretation and concluded that the band at  $\sim 2704$   $\text{cm}^{-1}$  (should be  $2717$   $\text{cm}^{-1}$ ) could be

considered 2D, the band at  $2944.5$   $\text{cm}^{-1}$  – D+G –  $\sim 2951$   $\text{cm}^{-1}$ ). With a large stretch, the band at  $3159$   $\text{cm}^{-1}$  can be interpreted as a 2D’ contribution ( $3532$   $\text{cm}^{-1}$ ). Therefore, it can be unequivocally stated that the available Raman spectra indicate a defective structure of the material.

In [33], the calculation of the particle thickness of graphene  $L_a$  by the following formula was proposed:

$$L_a(\text{nm}) = (2.4 \times 10^{-10}) \lambda_l^4 \left( \frac{I_D}{I_G} \right)^{-1} \quad (1)$$

where  $\lambda_l$  is the wavelength of the excitation radiation (in our case it is  $488$  nm),  $I_D$  is the intensity of the D-band,  $I_G$  is the intensity of the G-band. Given that the layers of GO have a thickness of about  $1.1 \pm 0.2$  nm according to [25, 26], we obtain that the thickness of GO particles is  $16$  nm, and the number of layers –  $15 \pm 1$  (corresponding to the certificate). This may be why the 2D band area is so wide and indistinct. Then for the reduced, nitrated and acid-modified GO the particle thicknesses will be  $10.5$ ,  $13.6$  and

12.4 nm. Thus, the reduction of GO makes the particles thinner, obviously, this does not change the number of layers, but changes the distance between the layers.

The particle size distribution was also determined using the dynamic light scattering method. Practically stable suspensions of GO and

its modified forms have a narrow monomodal particle size distribution (Fig. 5), which in the spherical approximation have the following average hydrodynamic diameters: GO  $\approx 1.5 \mu\text{m}$ , R-GO  $\approx 1.9 \mu\text{m}$ , N-GO  $\approx 2.3 \mu\text{m}$ , L-GO  $\approx 0.64 \mu\text{m}$ .

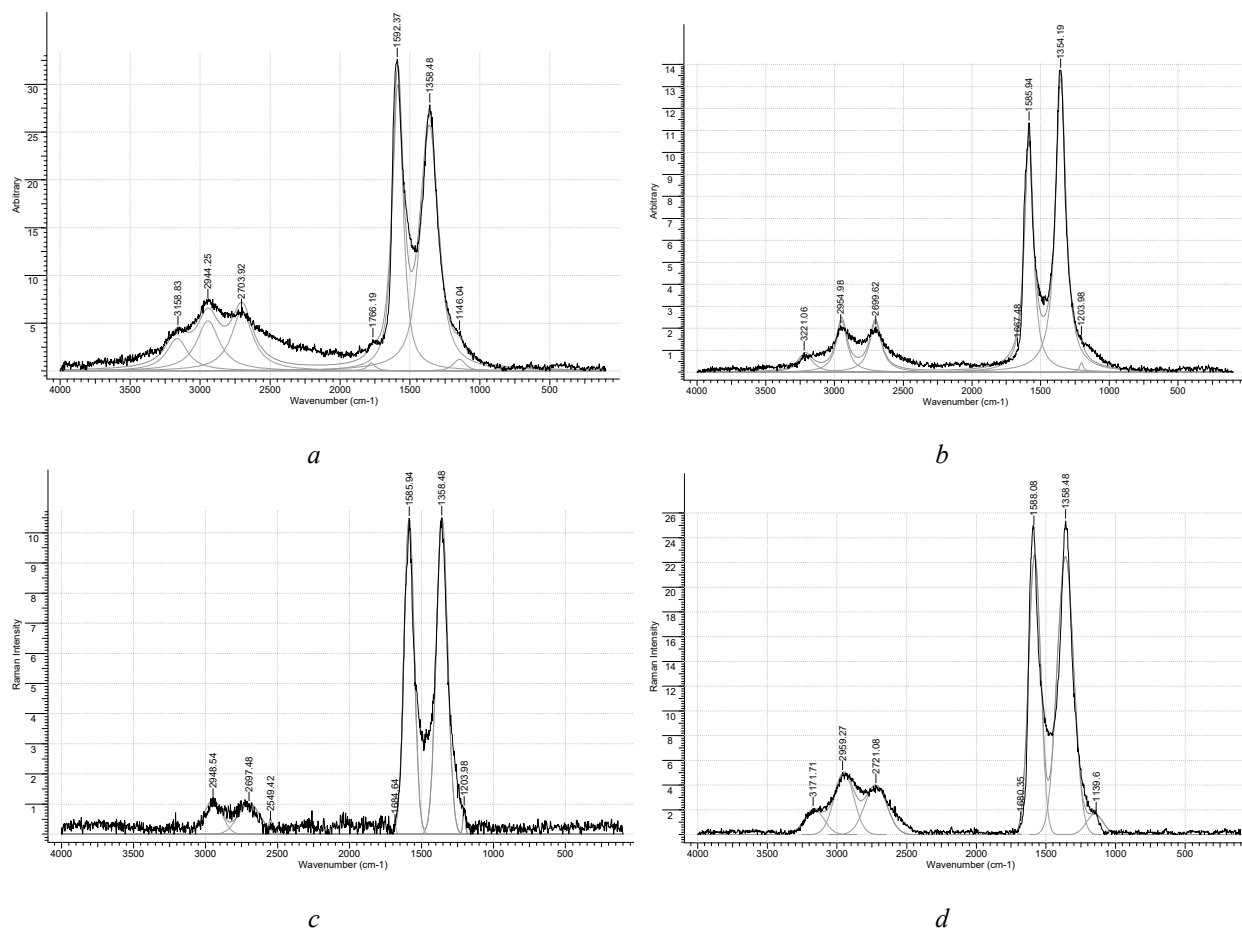


**Fig. 4.** Spectra of Raman scattering and deconvolution of these spectra in the form of Gauss-Lorentz bands after manual subtraction of the baseline: *a* – graphene oxide (source); *b* – reduced graphene oxide; *c* – nitrided; *d* – modified with *L*-cysteic acid

It is obvious that during modification the surface is hydrophobized in the case of reduced and nitrogen-containing samples, which may be accompanied by “sticking” of particles and increasing their hydrodynamic diameter. At the same time, modification with amino acids leads to a reduction of particles, which can affect their activity.

From the comparison of data for GO in different states, given in Table, the following conclusions can be drawn with some probability. Reduction of GO leads to a greater ordering of the structure of multilayer graphene relative to GO, as

evidenced by a decrease in the intensity of the  $sp^3$ -band (D (-)) (from 4.04 to 1.59 relative unit), shifting the frequencies of D and G bands in area of smaller values (from 1358.5 to 1354.2 cm<sup>-1</sup> and from 1592.4 to 1586.0 cm<sup>-1</sup>, respectively). Also, reduced by half the width of these lines (from 143.1 to 85.6 cm<sup>-1</sup> and from 110.40 to 77.6 cm<sup>-1</sup>). In this sense, the increase in the  $I_D/I_G$  ratio (from 0.82 to 1.3) looks rather strange, which usually corresponds to an increase in the disorder of the structure. N-doping of GO and modification of its by amino acid leads to the opposite effect – a slight deterioration of the structural state.

**Table.** The values of some basic parameters of the characteristic bands manifested in the micro-cattle of GO samples and its restored and modified forms and their values (\*) according to the results of deconvolution in the form of Gauss - Lorentz bands

No of sample	1	2	3	4
Synthesis conditions	GO-initial	R-GO	N-GO	L-GO(cysteic acid)
Shooting conditions	$\lambda=488 \text{ nm}, P=1 \text{ mW}, p3\lambda=488 \text{ nm}, P=1 \text{ mW}, p1\lambda=488 \text{ nm}, P=1 \text{ mW}, p2\lambda=488 \text{ nm}, P=1 \text{ mW}, p1$			
D, $\text{cm}^{-1}$	1358.5	1354.0	1358.5	1358.5
D(-), $\text{cm}^{-1}$	1146.7	1204.0	1204.0	1140.0
G, $\text{cm}^{-1}$	1592.4	1586.0	1586.0	1581.3
G(+), $\text{cm}^{-1}$	1766.2	–	–	–
D <sub>FWHM</sub> , $\text{cm}^{-1}$	172.3	109.6	137.7	139.8
G <sub>FWHM</sub> , $\text{cm}^{-1}$	104.6	105.3	111.3	94.3
2D <sub>1</sub> , $\text{cm}^{-1}$	2704.0	2700.0	2697.5	2721.0
2D <sub>2</sub> , $\text{cm}^{-1}$	2944.5	2955.0	2948.45	2959.0
2D <sub>3</sub> , $\text{cm}^{-1}$	3159.0	3221.0	–	3172.0
2D <sub>1FWHM</sub> , $\text{cm}^{-1}$	406.6	227.9	279.5	278.8
2D <sub>2FWHM</sub> , $\text{cm}^{-1}$	152.6	198.2	153.6	186.4
2D <sub>3 FWHM</sub> , $\text{cm}^{-1}$	181.4	126.3	–	157.4
I <sub>D</sub> , relative unit	23.7	11.9	9.6	23.0
I <sub>G</sub> , relative unit	29.0	9.2	9.5	20.3
I <sub>D</sub> /I <sub>G</sub>	0.82	1.3	1.0	1.1
I <sub>2D1</sub> /I <sub>G</sub>	0.12	0.14	0.1	0.17
I <sub>2D1</sub> , relative unit	3.5	1.3	0.9	3.4
I <sub>2D2</sub> , relative unit	3.0	1.4	0.8	4.1
I <sub>2D3</sub> , relative unit	2.0	0.3	–	1.7

Characterization of the surface of the samples was performed by the method of IR spectroscopy described above (Fig. 6).

The FTIR analysis shows that the GO surface has a large number of functional surface groups. The most characteristic peaks [34] for GO samples are observed at 3200–3400  $\text{cm}^{-1}$  (OH vibrations in alcohols), 1730  $\text{cm}^{-1}$  (C=O vibrations in carboxylic acids and aldehydes), 1620  $\text{cm}^{-1}$  (aromatic vibrations, C=C bonds), 1400  $\text{cm}^{-1}$  (OH vibrations in carboxylic acids), 1220  $\text{cm}^{-1}$  (C-O-C vibrations of epoxy groups), 1050  $\text{cm}^{-1}$  (CO-O-CO oscillations). The absorption band at 2100  $\text{cm}^{-1}$  corresponds to the overtone of weak C-H bonds in aromatic compounds.

The hydrazine reduction of GO completely hydrophobizes the surface, since almost all peaks corresponding to oxygen-containing functional groups disappear.

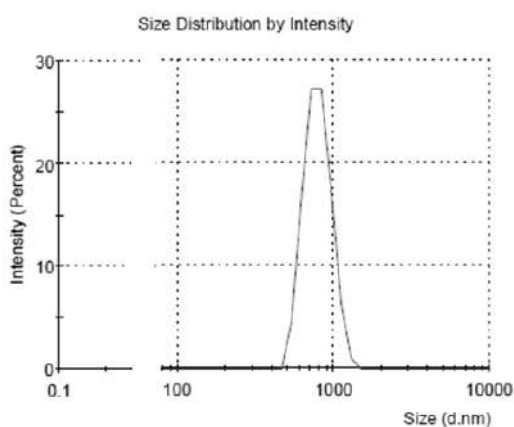
There is only a peak at  $\sim 1220 \text{ cm}^{-1}$ , which corresponds to C-O-C vibrations, and its intensity is significantly reduced. Adsorption band at 2100  $\text{cm}^{-1}$  which indicates the aromatic nature of the samples, remains in R-GO and N-GO derivatives. In addition, the new double-nature peak at 2300  $\text{cm}^{-1}$  that corresponds to the CO<sub>2</sub> adsorbed molecules appear in all samples. In N-GO and L-GO three peaks at 1730, 1400 and 1220  $\text{cm}^{-1}$  remain. Moreover, in N-GO the peak corresponding to the NH-stretching (2800  $\text{cm}^{-1}$ ) is appeared. Sulfur-containing derivatives have valence oscillations at 600  $\text{cm}^{-1}$  (data not shown), which most likely corresponds to S-H bonds and peak with wavelength at 790  $\text{cm}^{-1}$  (C-H and -HC=CH- bending).

The TPD-MS GO spectra (Fig. 7 a) indicate thermal decomposition of oxygen-containing functional groups that desorb in the form of water molecules ( $m/z$  17 and 18), CO<sub>2</sub> ( $m/z$  44), and CO ( $m/z$  28). Desorption peaks at  $\sim 120$  and

~ 180 °C indicate that GO decomposes at relatively low temperatures and has several layers. There is no peak with a mass of 32 (molecular oxygen), as well as physically adsorbed water ( $m/z$  17 and 18 at ~ 50 °C). The triple desorption peak is observed for all masses and indicates the diversity of functional groups on the GO surface. The first peak at ~ 120 °C, the second at 160 °C and the last at 180 °C. Masses

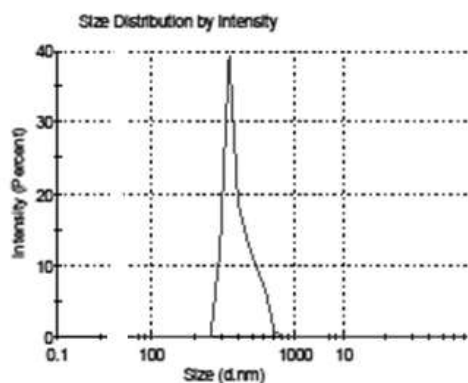
17 and 18 at ~ 120 °C belong to chemically bound water, while at ~ 160–180 °C – with OH groups from oxygen-containing functional groups (including carboxyl and phenolic). Masses 28 and 44 correspond to O-containing surface groups. TPD-MS spectra of GO derivatives (Fig. 7 *b, c, d*) indicate a significant change in surface functional groups and essentially confirm the data obtained by IR spectroscopy.

	Size (d.n...	% Intensity:	St Dev (d.n...
Peak 1:	790,6	100,0	153,2
Z-Average (d.nm): 1531			



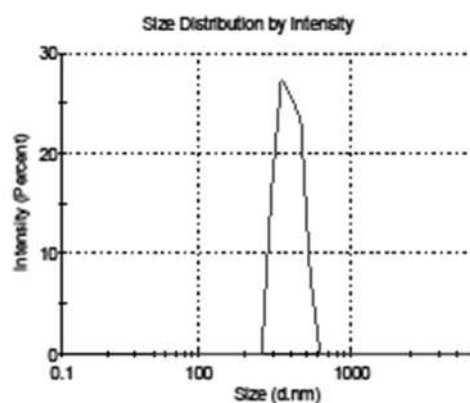
*a*

	Size (d.n...	% Intensity:	St Dev (d.n...
Peak 1:	399,6	100,0	91,04
Z-Average (d.nm): 2332			



*c*

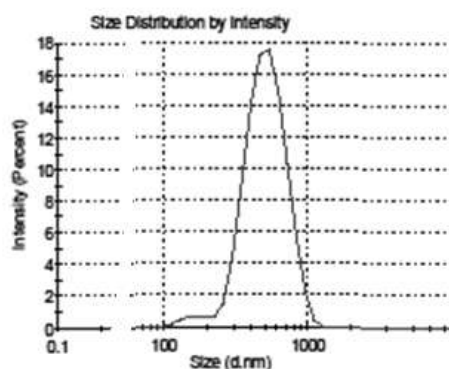
	Size (d.n...	% Intensity:	St Dev (d.n...
Peak 1:	390,2	100,0	68,78
Z-Average (d.nm): 1925			



*b*

	Size (d.n...	% Intensity:	St Dev (d.n...
Peak 1:	522,5	97,6	162,6
Peak 2:	155,8	2,4	26,02
Z-Average (d.nm): 645,4			

PdI: 0,477



*d*

**Fig. 5.** Particle distribution by radius (*a*) – GO, (*b*) – R-GO, (*c*) – N-GO, (*d*) – L-GO

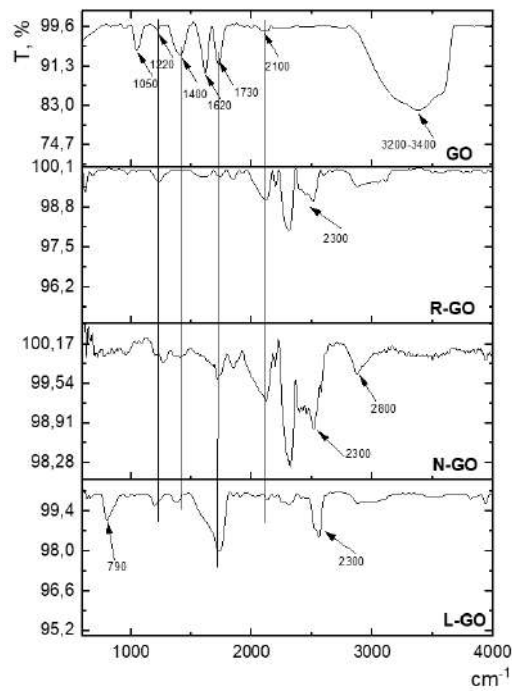


Fig. 6. IR spectra of obtained samples

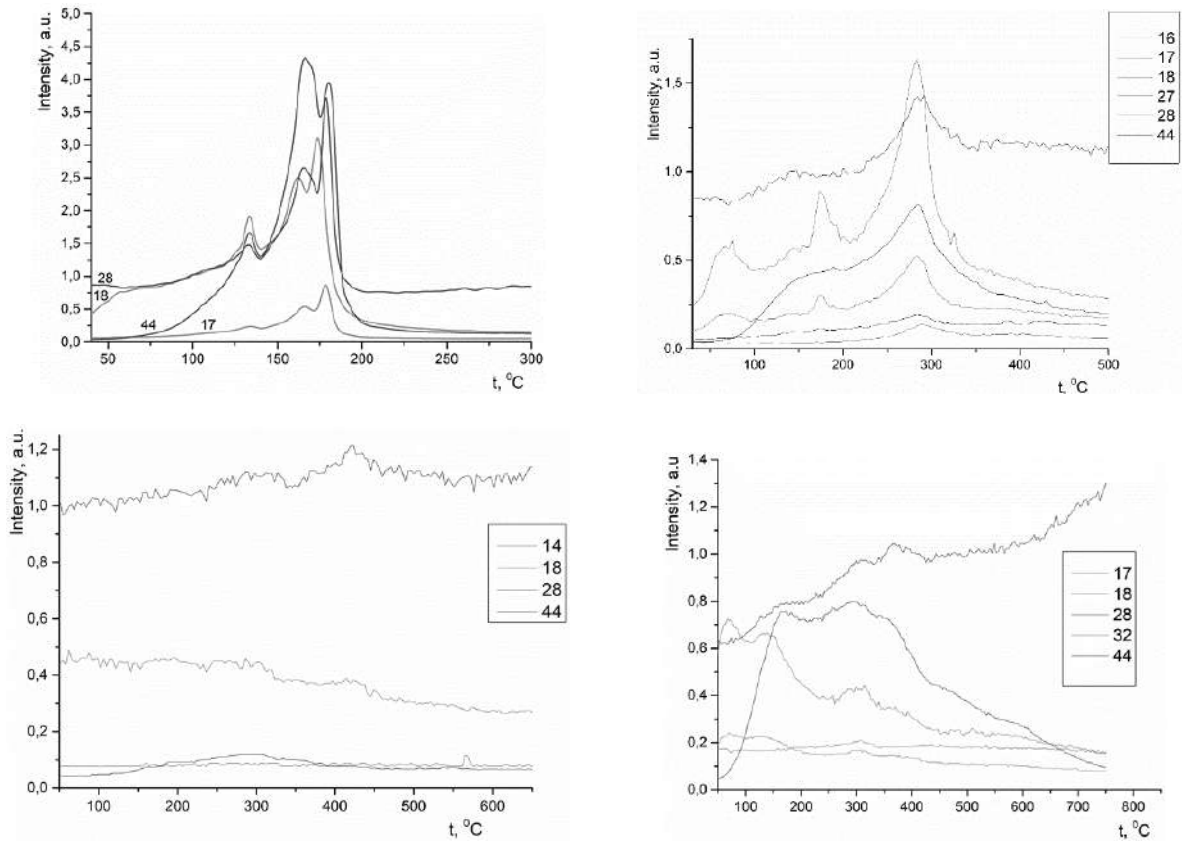


Fig. 7. TPD-MS spectra: (a) – GO, (b) – R-GO, (c) – N-GO, (d) – L-GO



## CONCLUSION

Comprehensive studies conducted by Raman, DLS, IR spectroscopy, thermo-programmed mass spectroscopy have shown that the reduction of graphene oxide with hydrazine hydrate, its modification with nitrogen by impregnation with urea and subsequent heat treatment and sulfur-containing compound obtained by the addition of L-cysteic acid are effective, lead to significant changes in its structure and surface chemistry. Empirical studies [37] have shown that such

changes affect the capability of the obtained samples to scavenge free radicals and this property increases in a row:



*Authors are grateful to "Grafren AB" for the GrO sample with the highest purity synthesis; to G.I. Dovbeshko for interpretation of the RAMAN spectra.*

*This work was funded by the National Research Foundation of Ukraine (project number 2020.01/0107).*

### Зміна структури та стану поверхні оксиду графену за його відновлення та модифікування

**М.Т. Картель, К.В. Войтко, Ю.В. Гребельна, С.В. Журавський, К.О. Іваненко,  
Т.В. Кулик, С.М. Махно, Ю.І. Семенцов**

*Ningbo Sino-Ukrainian New Materials Industrial Technologies Institute  
Kechuang building, N777 Zhongguan road, Ningbo, 315211, China  
Ningbo University of Technology*

*No 55-155 CuiBaiRoad, Ningbo, 315016, China*

*Інститут хімії поверхні ім. О.О. Чуйка Національної академії наук України  
бул. Генерала Наумова, 17, Київ, 03164, Україна, ysementsov@ukr.net*

*Інститут хімії високомолекулярних сполук Національної академії наук України  
Харківське шосе, 48, Київ, 02160, Ukraine*

Метою поточного дослідження було встановити зміни структури та стану поверхні оксиду графену (GO) за умов його відновлення та модифікування гетероатомами азоту та амінокислотою. Відновлення GO проводилось гідратом гідразину (R-GO), допування атомами азоту - просоченням сечовиною та подальшою термообробкою (N-GO), а також поверхню GO модифікували сірковмісною амінокислотою – L-цистеїном нуклеофільним приєднанням (L-GO). Отримані зразки були охарактеризовані аналітичними методами, такими як комбінаційне розсіяння світла (КРС), ІЧ-спектроскопія, ТПД-мас-спектрометрія, спектроскопія динамічного світлорозсіювання. Наявні КР спектри свідчать про дефектну структуру GO, відновлення GO призводить до більшого упорядкування структури по відношенню до GO, азотування та модифікування амінокислотою - до протилежного ефекту, незначного погіршення структурного стану. За результатами ІЧ-спектроскопії, підтверджених також ТПД-МС, GO має велику кількість функціональних поверхневих груп: (OH), (C=O), (C=C), (C-O-C), (CO-O-CO), (C-H). Відновлення гідратином повністю гідрофобізує поверхню, в ІЧ-спектрах лишається лише пік при  $\sim 1040 \text{ см}^{-1}$ , що відповідає CO-O-CO коливанням, з істотно зниженою інтенсивністю, а також смуги при 2120 та 2300  $\text{см}^{-1}$ , які свідчать про ароматичну природу зразків й існують в усіх похідних GO. В азот- та сірковмісних зразках (L-GO) з'являється новий пік  $\sim 1520 \text{ см}^{-1}$ , що відповідає N-H коливанням в амінах. Сірковмісні похідні мають валентні коливання при 600  $\text{см}^{-1}$ , що найімовірніше відповідає S-H зв'язкам. Таким чином, модифікування GO призводить до суттєвої зміни його структури та хімії поверхні, що в свою чергу впливає на здатність отриманих зразків уловлювати вільні радикали. Попередні емпіричні дослідження показали, що така властивість зростає в ряду L-GO > GO > N-GO > R-GO.

**Ключові слова:** оксид графену, структура, властивості поверхні

## REFERENCES

1. He H., Klinowski J., Forster M., Lerf A. A new structural model for graphite oxide. *Chem. Phys. Lett.* 1998. **287**(1): 53.
2. Hummers W.S., Offeman R.E. Preparation of Graphitic Oxide. *J. Am. Chem. Soc.* 1958. **80**(6): 1339.
3. Sadri R., Kamali K.Z., Hosseini M., Zubir N., Kazi S.N., Ahmadi G., Dahari M., Huang N.M., Golsheikh A.M. Experimental study on thermo-physical and rheological properties of stable and green reduced graphene oxide nanofluids: Hydrothermal assisted technique. *J. Dispersion Sci. Technol.* 2017. **38**(9): 1302.
4. Dreyer D.R., Park S., Bielawski C.W., Ruoff R.S. The chemistry of graphene oxide. *Chem. Soc. Rev.* 2010. **39**(1): 228.
5. Wei X.-D., Mao L., Soler-Crespo R.A., Paci J.T., Huang J.-X., Nguyen S.T., Espinoza H.D. Plasticity and ductility in graphene oxide through a mechanochemically induced damage tolerance mechanism. *Nat. Commun.* 2015. **6**: 8029.
6. Rawat P.S., Srivastava R.C., Dixit G., Asokan K. Structural, functional and magnetic ordering modifications in graphene oxide and graphite by 100 MeV gold ion irradiation. *Vacuum.* 2020. **182**: 109700.
7. Brodie B.C. On the Atomic Weight of Graphite. *Philos. Trans. R. Soc. London.* 1859. **149**: 249.
8. Kumar H.V., Woltornist S.J., Adamson D.H. Fractionation and Characterization of Graphene Oxide by Oxidation Extent Through Emulsion Stabilization. *Carbon.* 2016. **98**: 491.
9. Feicht P., Siegel R., Thurn H., Neubauer J.W., Seuss M., Szabó T., Talyzin A.V., Halbig C.E., Eigler S. Systematic evaluation of different types of graphene oxide in respect to variations in their in-plane modulus. *Carbon.* 2017. **114**: 700.
10. Boehm H.-P., Scholz W. Der "Verpuffungspunkt" des Graphitoxids. *Zeitschrift für Anorganische und Allgemeine Chemie.* 1965. **335**(1–2): 74.
11. You S., Luzan S.M., Szabó T.S., Talyzin A.V. Effect of synthesis method on solvation and exfoliation of graphite oxide. *Carbon.* 2013. **52**: 171.
12. Pei S., Wei Q., Huang K., Cheng H.-M., Ren W. Green synthesis of graphene oxide by seconds times scale water electrolytic oxidation. *Nat. Commun.* 2018. **9**: 145.
13. Amani H., Habibey R., Hajmiresmail S.J., Latifi S., Pazoki-Toroudi H., Akhavan O. Antioxidant nanomaterials in advanced diagnoses and treatments of ischemia reperfusion injuries. *J. Mater. Chem. B.* 2017. **5**(48): 9452.
14. Maddu N. Diseases Related to Types of Free Radicals. In: *Antioxidants*. (IntechOpen, 2019).
15. Gao L.Z., Zhuang J., Nie L., Zhang J.B., Zhang Y., Gu N., Wang T.H., Feng J., Yang D.L., Perrett S., Yan X. Intrinsic peroxidase-like activity of ferromagnetic nanoparticles. *Nat. Nanotechnol.* 2007. **2**(9): 577.
16. Lin Y.H., Ren J.S., Qu X.G. Nano-Gold as Artificial Enzymes: Hidden Talents. *Adv. Mater.* 2014. **26**(25): 4200.
17. Wang G.L., Xu X.F., Qiu L., Dong Y.M., Li Z.J., Zhang C. Dual Responsive Enzyme Mimicking Activity of AgX (X = Cl, Br, I) Nanoparticles and Its Application for Cancer Cell Detection. *ACS Appl. Mater. Interfaces.* 2014. **6**(9): 6434.
18. Hu A.L., Liu Y.H., Deng H.H., Hong G.L., Liu A.L., Lin X.H., Xia X.H., Chen W. Fluorescent hydrogen peroxide sensor based on cupric oxide nanoparticles and its application for glucose and L-lactate detection. *Biosens. Bioelectron.* 2014. **61**: 374.
19. Nia Z.K., Chen J.Y., Tang B., Yuan B., Wang X.G., Li J.L. Optimizing the free radical content of graphene oxide by controlling its reduction. *Carbon.* 2017. **116**: 703.
20. Qiu Y., Wang Z.Y., Owens A.C.E., Kulaots I., Chen Y.T., Kane A.B., Hurt R.H. Antioxidant chemistry of graphene-based materials and its role in oxidation protection technology. *Nanoscale.* 2014. **6**(20): 11744.
21. Stankovich S., Dikin D.A., Piner R.D., Kohlhaas K.A., Kleinhammes A., Jia Y., Wu Y., Nguyen S.B.T., Ruoff R.S. Synthesis of graphene-based nonosheets via chemical reduction of exfoliated graphite oxide. *Carbon.* 2007. **45**: 1558.
22. Ng H.H., Yildiz G.S., Ku J.M., Miller A.A., Woodman O.L., Hart J.L. Chronic NaHS treatment decreases oxidative stress and improves endothelial function in diabetic mice. *Diab. Vasc. Dis. Res.* 2017. **14**(3): 246.
23. Askari H., Seifi B., Kadkhodae M., Sanadgol N., Elshiekh M., Ranjbaran M., Ahghari P. Protective effects of hydrogen sulfide on chronic kidney disease by reducing oxidative stress, inflammation and apoptosis. *EXCLI J.* 2018. **17**: 14.
24. Shymans'ka T.V., Hoshovs'ka Iu.V., Semenikhina O.M., Sagach V.F. Effect of hydrogen sulfide on isolated rat heart reaction under volume load and ischemia-reperfusion. *Fiziol Zh.* 2012. **58**(6): 57.
25. Pandey D., Reifengerger R., Piner R. Scanning probe microscopy study of exfoliated oxidized graphene sheets. *Surf. Sci.* 2008. **602**(9): 1607.
26. Mkhoyan K.A., Contryman A.W., Silcox J., Stewart D.A., Eda G., Mattevi C., Miller S., Chhowalla M. Atomic and Electronic Structure of Graphene-Oxide. *Nano Lett.* 2009. **9**(3): 1058.

27. Schniepp H.C., Li J.L., McAllister M.J., Sai H., Herrera-Alonso M., Adamson D.H., Prud'Homme R.K., Car R., Saville D.A., Aksay I.A. Functionalized Single Graphene Sheets Derived from Splitting Graphite Oxide. *J. Phys. Chem. B*. 2006. **110**(17): 8535.
28. Raval S. *Ultrafast Pump-Probe spectroscopy of Graphene Oxide (GO) and Reduced Graphene Oxide (RGO)*. Thesis for Master of Science. (Indian Institute of Technology Kharagpur, 2018).
29. Stankovich S., Piner R.D., Chen X., Wu N., Nguyen S.T., Ruoff R.S. Stable aqueous dispersions of graphitic nanoplatelets via the reduction of exfoliated graphite oxide in the presence of poly(sodium 4-styrenesulfonate). *J. Mater. Chem.* 2006. **16**(2): 155.
30. Yamada Y., Yasuda H., Murota K., Nakamura M., Sodesawa T., Sato S. Analysis of heat-treated graphite oxide by X-ray photoelectron spectroscopy. *J. Mater. Sci.* 2013. **48**(23): 8171.
31. Kudin K.N., Ozbas B., Schniepp H.C., Prud'homme R.K., Aksay I.A., Car R. Raman Spectra of Graphite Oxide and Functionalized Graphene Sheets. *Nano Lett.* 2008. **8**(1): 36.
32. Bokobza L., Bruneel J.-L., Couzi M. Raman Spectra of Carbon-Based Materials (from Graphite to Carbon Black) and of Some Silicone Composites. *Carbon*. 2015. **2015**(1): 77.
33. Cancado L.G., Takai K., Enoki T., Endo M., Kim Y.A., Mizusaki H., Jorio A., Coelho L.N., Magalhães-Paniago R., Pimenta M.A. General equation for the determination of the crystallite size  $L_a$  of nanographite by Raman spectroscopy. *Appl. Phys. Lett.* 2006. **88**(16): 163106.
34. Rattana T., Chaiyakun S., Witit-anun N., Nuntawong N., Chindaudom P., Oaew S., Kedkeaw C., Limsuwan P. Preparation and characterization of graphene oxidenanosheets. *Procedia Eng.* 2012. **32**: 759.
35. Nedilko S.G., Revo S.L., Chornii V., Scherbatskyi V., Ivanenko K., Nediuko M., Sementsov Yu., Skoryk M., Nikolenko A., Strelchuk V. Structure and Optical Features of Micro/Nanosized Carbon Forms Prepared by Electrochemical Exfoliation. *Nanoscale Res. Lett.* 2017. **12**: 28.
36. Kartel M., Sementsov Yu., Dovbeshko G., Karachevtseva L., Makhno S., Aleksyeyeva T., Grebelna Y. Lamellar structures from graphene nanoparticles produced by anode oxidation. *Adv. Mater. Lett.* 2017. **8**(3): 212.
37. Voitko K.V., Bakalinska O.M., Sementsov Yu.I., Goshovska Yu.V. Perspectives of the usage of nano-antioxidants for cardiovascular diseases therapy. Book of Abstract Ukrainian Conference with International Participation Chemistry, Physics and Technology of Surface Devoted to the 35<sup>th</sup> Anniversary of the Chuiko Institute of Surface Chemistry of NAS of Ukraine and Workshop Nano-Structures and Nanomaterials in Medicine: Challenges, Tasks and Perspectives. 26-27 May 2021, Kyiv, Ukraine. P. 212.

Received 10.12.2021, accepted 01.06.2022